Static and Dynamic Analysis of Magnetic Tunnel Junctions With Wedged MgO Barrier

Static and dynamic analysis of magnetic tunnel junctions with wedged MgO barrier

Ambra Caprile[1], Alessandra Manzin[1], Marco Coïsson[1], Massimo Pasquale[1], Hans W. Schumacher[2], Niklas Liebing[2], Sybille Sievers[2], Ricardo Ferreira[3], Santiago Serrano-Guisan[3]

[1]Istituto Nazionale di Ricerca Metrologica (INRIM), Torino, 10135, Italy
[2] Physikalisch-Technische Bundesanstalt (PTB), Braunschweig, 38116, Germany
[3]International Iberian Nanotechnology Laboratory (INL), Braga, 4715-330, Portugal

This paper deals with the experimental characterization of CoFeB based magnetic tunnel junctions with wedged MgO barrier. We perform both static hysteresis loop measurements by means of an alternating gradient force magnetometer and magnetization dynamics analysis via vector network analyzer ferromagnetic resonance spectroscopy in a wide field range. The results, supported by a simplified model based on coherent rotation assumption, put in evidence the role of the tunnel barrier thickness on the exchange coupling between free and reference layers. In presence of strong ferromagnetic interaction, the easy-axis hysteresis loop does not exhibit the typical low-field plateau associated to antiparallel alignment, indicating a simultaneous reversal of the two layers. Moreover, a stronger asymmetry is observed in the ferromagnetic resonance spectrum at low bias fields.

***Index Terms*—Magnetic tunnel junctions, static hysteresis loops, ferromagnetic resonance, exchange coupling.**

I. Introduction

Recently, there has been a growing interest in spin transfer torque magnetic random access memories (ST-MRAMs) made of magnetic tunnel junction (MTJ) cells [1]. Such applications are based on the injection of high-density spin-polarized currents, which induce spin torque precession of the magnetization in the MTJ free layer, leading to its possible reversal. The switching behavior and the magnetic stability of these devices are strongly affected by the magnetic properties of the constituent layers, as well as by their interaction mechanisms [2].

One of the fundamental parameters for ST-MRAM applications is the thickness of the MTJ tunneling barrier, which has an impact on both tunneling magnetoresistance ratio and resistance-area product. Moreover, it determines the strength of the exchange coupling between the free and reference layers, influencing in turn the effective damping coefficient of the free layer and thus the critical current density for ST magnetization reversal [3, 4].

In this framework, we study CoFeB based MTJs with a wedged MgO tunneling barrier with variable thickness, nominally ranging from 0.4 nm to 0.98 nm. The experimental analysis focuses on static hysteresis loop measurements by means of an alternating gradient force magnetometer (AGFM), as well as on magnetization dynamics characterization via vector network analyzer ferromagnetic resonance spectroscopy (VNA-FMR). Analytical models based on macro-spin approximation have been developed to interpret both the static and dynamic behavior of MTJs, in dependence on the tunnel barrier thickness and exchange coupling between the free and reference layers.

Manuscript received June 13, 2014. Corresponding author: A. Caprile (e-mail: a.caprile@inrim.it).
Digital Object Identifier inserted by IEEE

II. Sample Description

The samples are obtained from a stack with an MgO wedge shaped tunneling barrier with thickness t_{MgO}. The stack contains two CoFeB layers spaced by the MgO barrier, i.e. the free (FL) and reference (RL) layer. A pinned layer (PL) made of CoFe is separated from RL by a Ru coupling layer. An IrMn antiferromagnetic pinning layer (AF) is located below PL. The complete layer sequence is: Ta(5)/ CuN(50)/ Ta(5)/ CuN(50)/ Ta(5)/ Ru(5)/ IrMn(20)/ $Co_{70}Fe_{30}$(2)/ Ru(0.85)/ $Co_{40}Fe_{40}B_{20}$(2.6)/ MgO(t_{MgO})/ $Co_{40}Fe_{40}B_{20}$(2)/ Ta(10)/ Ru(7) from bottom to top, where the numbers in parentheses indicate the layer thickness in nm.

The stack is deposited on a 18 cm diameter Si/Al_2O_3 wafer and annealed at 330 °C for two hours with a field of 1 T to enforce the exchange bias orientation. Then, it is cut into (3×4) mm^2 samples with variable tunneling barrier thickness (being the wedge slope 0.003 nm/mm, the variation of t_{MgO} over the size of the single piece can be neglected). The insulating layer thickness has been obtained in an indirect way through the measurement of the resistance-area product, which shows an exponential decay with decreasing t_{MgO} [3]. The ferromagnetic layers are characterized by in-plane anisotropy, with easy axis parallel to the exchange-biasing direction.

III. Static Hysteresis Loops

The static hysteresis loops of the obtained samples are first measured by means of an AGFM, sweeping the external field between saturation states (± 700 mT).

The results of the measurements performed with the external field applied along the easy axis (in-plane) are reported in Fig. 2a, considering samples with different MgO barrier thickness, ranging from 0.4 nm to 0.98 nm. Generally, the devices with higher t_{MgO} show three distinguishable sub-loops, associated with the distinctive reversal of the magnetization in the three ferromagnetic layers [5, 6]. Sub-

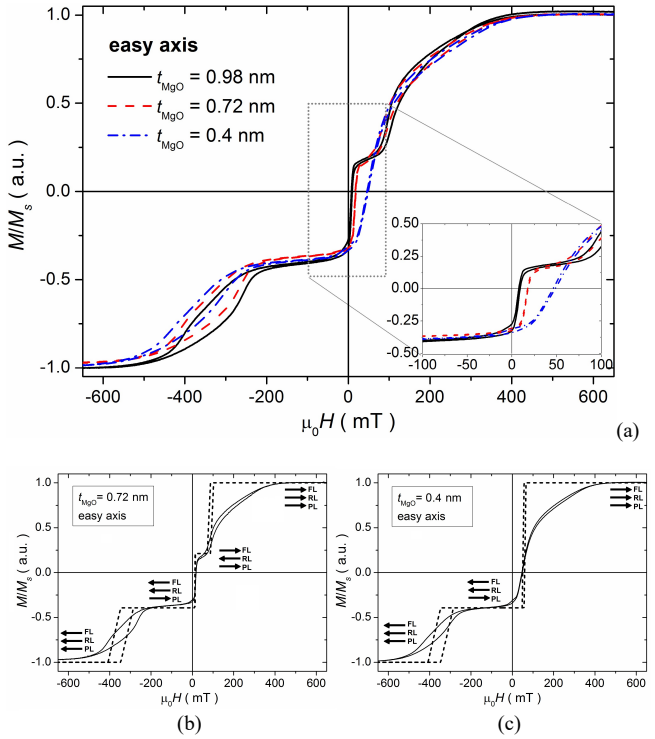

Fig. 2. (a) AGFM measurements of the easy-axis hysteresis loops of MTJs with different thicknesses of the MgO tunneling barrier, ranging from 0.4 nm to 0.98 nm. Modeled normalized magnetization of the system (dashed lines) versus applied field for (b) t_{MgO} = 0.72 nm and (c) t_{MgO} = 0.4 nm (strong coupling), compared to experimental data (solid lines). The schemes indicate the relative orientation of the magnetization in the ferromagnetic layers.

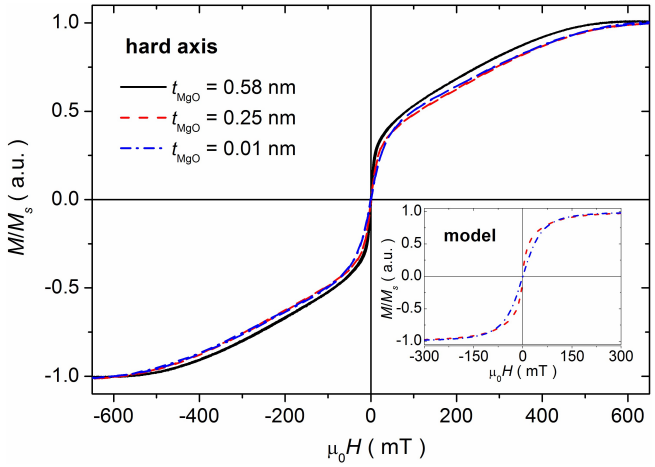

Fig. 3. AGFM measurements of the hard-axis hysteresis loops of MTJs with different thicknesses of the MgO tunneling barrier, ranging from 0.4 nm to 0.98 nm. In the inset: modeled normalized magnetization of the system versus applied field for t_{MgO} equal to 0.72 nm and 0.4 nm (strong coupling).

loop #1 corresponds to the switching in RL, while sub-loop #2, manifesting itself at very low fields, results from the magnetization reversal in FL. Sub-loop #3, at negative fields, is associated with the switching in PL.

For the sample with the lowest MgO barrier thickness, there are only two sub-loops, i.e. there is no distinction between the switching behaviors of RL and FL. This is consistent with the fact that for a very small barrier thickness, the relative exchange coupling is so strong that the two layers actually behave as a single layer, shifting FL reversal towards higher external fields. Moreover, the intrinsic presence of micro-structural fluctuations and pinholes in the insulating layer contributes to a further increase in the RL-FL coupling.

The AGFM results are interpreted by an analytical model based on the assumption that the magnetization in the ferromagnetic layers is distributed uniformly in the *x*-*y* plane, rotating with a coherent motion [7]. Specifically, the shifts of the three ferromagnetic layer sub-loops are extracted from the stability conditions of the following expression for the total magnetic free energy density:

$$E = -\mu_0 M_{FL} H \cos(\phi_H - \phi_{FL}) - k_{FL} \cos^2(\phi_{FL}) - \frac{J_{FL}}{t_{FL}} \cos(\phi_{RL} - \phi_{FL})$$
$$-\mu_0 M_{RL} H \cos(\phi_H - \phi_{RL}) - k_{RL} \cos^2(\phi_{RL}) - \frac{J_{AF}}{t_{RL}} \cos(\phi_{RL} - \phi_{PL})$$
$$-\mu_0 M_{PL} H \cos(\phi_H - \phi_{PL}) - k_{PL} \cos^2(\phi_{PL}) - \frac{J_{ex}}{t_{PL}} \cos(\phi_{PL} - \phi_{AF})$$
$$-k_{AF} \cos^2(\phi_{AF}) \qquad (1)$$

where $M_{FL/RL/PL}$ indicates the magnetization saturation of the corresponding layer (AF has negligible magnetic moment), $k_{FL/RL/PL}$ its anisotropy constant and $t_{FL/RL/PL}$ its thickness; J_{FL} is the exchange coupling between FL and RL, J_{AF} is the antiferromagnetic interlayer exchange coupling between RL and PL, J_{ex} is the exchange bias coupling between PL and AF, while ϕ_{FL}, ϕ_{RL}, ϕ_{PL} and ϕ_{AF} are the angles between the magnetization vector in the layers and the easy axis. The applied field makes an angle ϕ_H with respect to the easy axis. When $\phi_H = 0$, the sub-loop shifts predicted by the model are

$$H_{RL} = -\frac{1}{\mu_0 M_{RL}} \left(\frac{J_{AF}}{t_{RL}} + \frac{J_{FL}}{t_{FL}} \right)$$
$$H_{FL} = \frac{J_{FL}}{\mu_0 M_{FL} t_{FL}} \qquad (2)$$
$$H_{PL} = \frac{1}{\mu_0 M_{PL}} \left(\frac{J_{AF}}{t_{RL}} - \frac{J_{ex}}{t_{PL}} \right)$$

In particular, the easy-axis hysteresis loop of the sample with t_{MgO} = 0.72 nm can be approximated by considering the following parameters: $\mu_0 M_{FL}$ = (0.82 ± 0.01) T, J_{FL} = (17.0 ± 0.5) μJ/m^2 and J_{AF} = (-170 ± 10) μJ/m^2. The low saturation magnetization of CoFeB, which can lead to a decrease in the critical current density for ST switching [8], is a consequence of both reduced layer thickness [9] and Ta capping layer presence [10]. The calculated normalized magnetization is plotted versus the applied magnetic field in Fig. 2b, where it is compared to the measured cycle. The model is able to well reproduce the sub-loop shifts, but not the shape of the experimental cycles, which exhibit smooth magnetization switching. This effect can be ascribed to the formation of complex magnetization patterns within the ferromagnetic layers, such as domain-wall nucleation and propagation. Such processes, energetically favored by edge roughness or local defects, can be described by micromagnetic simulations [11], here not possible due to the large extension of the samples.

For higher values of t_{MgO} there is a weaker exchange coupling between FL and RL, represented by a lower value of

J_{FL}, which explains the shift in the FL sub-loop towards zero and the increase in H_{RL}, as observed when t_{MgO} = 0.98 nm (black curve in Fig. 2a).

On the contrary, the results obtained with low MgO barrier thickness can be interpreted by treating FL and RL as a unique layer with saturation magnetization and anisotropy constant respectively given by $\frac{M_{FL}t_{FL}+M_{RL}t_{RL}}{t_{FL}+t_{RL}}$ and $\frac{k_{FL}t_{FL}+k_{RL}t_{RL}}{t_{FL}+t_{RL}}$, and with antiferromagnetic coupling field reduced to $\frac{J_{AF}}{\mu_0\left(M_{FL}t_{FL}+M_{RL}t_{RL}\right)}$. As a consequence, the reversal in the CoFeB layers takes place in correspondence of a shifted field intermediate between the previously estimated values for H_{RL} and H_{FL} (Fig. 2c).

As shown in Fig. 3, a different behavior is observed in the hysteresis loops measured along the hard-axis direction. In this case, sub-loops are not visible and the cycles are almost zero-hysteretic for all the samples, as also seen in [5], where the coercive fields of the magnetic layers reduce with increasing the angle between the applied field and the biasing direction of PL. The theoretical model has been also applied to interpret the results obtained for the hard-axis measurements (the calculated curves are reported in the inset of Fig. 3). Under the assumption of weak FL - RL coupling, the angles between the magnetization vectors in FL and RL and the easy axis can be approximated as

$$\phi_{FL} = arctg\left(\mu_0 M_{FL} H \frac{t_{FL}}{J_{FL}}\right)$$
$$\phi_{RL} = arctg\left[\left(\mu_0 M_{RL} H + \frac{J_{FL}}{t_{FL}}\right)\frac{t_{RL}}{|J_{AF}|}\right] \quad (3)$$

The switching in FL takes place between -50 mT and 50 mT, while the magnetization rotation in RL covers the entire field range. The thickness of the MgO barrier has a reduced impact, influencing parameter J_{FL} only. For strong coupling (t_{MgO} = 0.4 nm), the two CoFeB layers can again be treated as an equivalent one, leading to a more gradual reversal, as found experimentally.

IV. Ferromagnetic Resonance Characterization

The dynamic magnetic behavior of the considered MTJs is characterized with the VNA-FMR technique, which provides the frequency spectrum of the system magnetic permeability for a specific applied external field [12]. The measurements have been performed with a Rhode-Schwarz VNA in the frequency sweep mode from 1 GHz to 18 GHz at a fixed power of 1 mW, with the field varying in a wide range from -180 mT to 180 mT.

The map in Fig. 4a shows the static field dependence of the measured ferromagnetic resonance spectra for the device with tunneling barrier thickness t_{MgO} = 0.72 nm and bias field applied along the easy-axis direction, putting in evidence the absorption peak position. The corresponding resonance frequency f_{FMR} can be fitted (open circles) by the following relationship, derived from Smit and Beljers formula [13]

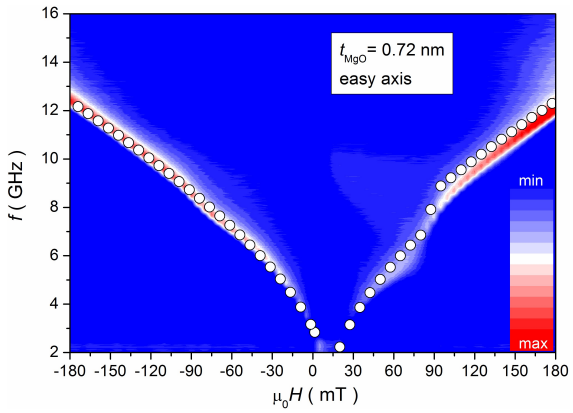

(a)

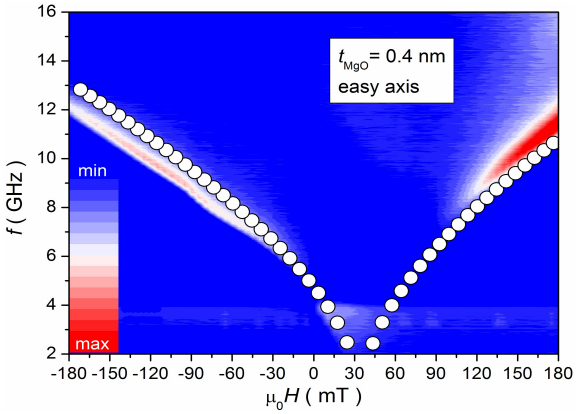

(b)

Fig. 4. (a) VNA-FMR maps of the static field dependence of ferromagnetic resonance spectra for the MTJs with (a) t_{MgO} = 0.72 nm and (b) t_{MgO} = 0.4 nm, considering a bias field applied along the easy-axis direction. The calculated ferromagnetic resonance curves are represented by open circles.

$$f_{FMR} = \frac{\gamma\mu_0}{2\pi}\sqrt{\frac{J_{FL}}{t_{FL}\left(\mu_0 M_{FL}\right)}\cos\left(\phi_{FL}-\phi_{RL}\right)+\frac{2k_{FL}}{\mu_0 M_{FL}}\cos\left(2\phi_{FL}\right)+H\cos\left(\phi_{FL}-\phi_H\right)}\cdot \quad (4)$$
$$\sqrt{\frac{J_{FL}}{t_{FL}\left(\mu_0 M_{FL}\right)}\cos\left(\phi_{FL}-\phi_{RL}\right)+\frac{2k_{FL}}{\mu_0 M_{FL}}\cos^2\left(\phi_{FL}\right)+H\cos\left(\phi_{FL}-\phi_H\right)+M_{FL}}$$

where γ is the gyromagnetic factor. The fitting has been performed by considering the same parameter values used in the hysteresis loop reconstruction.

The jump in the positive field branch at ~ 85 mT, well reproduced by the model, is associated with the RL magnetization reversal. In particular, it depends on the exchange coupling between FL and RL, as well as on the antiferromagnetic coupling between RL and PL, since

$$\phi_{RL} = arc\cos\left[\left(\mu_0 M_{RL} H + \frac{J_{FL}}{t_{FL}} + \frac{J_{AF}}{t_{RL}}\right)\frac{1}{2k_{RL}}\right]. \quad (5)$$

The small shift in the resonance frequency with respect to the bias field (with amplitude of ~ 15 mT) is a consequence of the weak FL-RL ferromagnetic coupling described by J_{FL} [14]. When considering higher MgO layer thicknesses, this shift reduces and, contemporary, a small increase in the resonance frequency can be found at low fields. On the contrary, in presence of strong coupling the jump in the positive field branch associated with RL switching disappears (Fig. 4b). Moreover, there is an increase in the asymmetry of the precession frequency with respect to zero field, corresponding

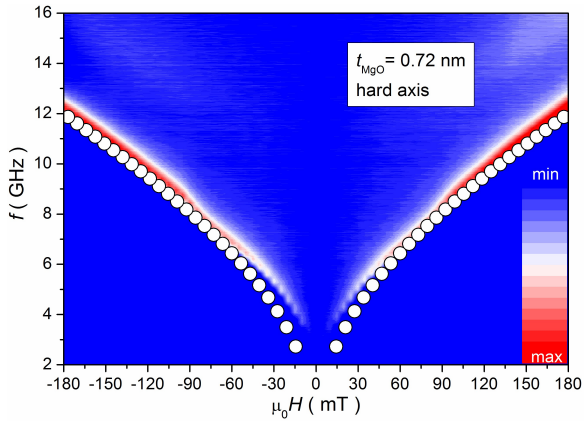

Fig. 5. VNA-FMR map of the static field dependence of ferromagnetic resonance spectra for the MTJ with t_{MgO} = 0.72 nm, considering a bias field applied along the hard-axis direction. The calculated ferromagnetic resonance curve is represented by open circles.

to the shift in the FL reversal at higher fields. These effects can be simulated by treating FL and RL as a unique layer [15], as previously done for the interpretation of the static hysteresis loop in Fig. 2c. In this case, the shift in f_{FMR} is strongly influenced by the antiferromagnetic interlayer exchange coupling between RL and PL J_{AF}.

The strong ferromagnetic coupling between FL and RL leads to a modification of the effective damping coefficient α_{eff}, which can be extracted from the linewidth of the FMR peak [16]. For the lowest value of t_{MgO}, we have estimated $\alpha_{eff} = 0.020 \pm 0.005$, including in the effective field the equivalent antiferromagnetic coupling term. For higher thicknesses, we have found $\alpha_{eff} = 0.010 \pm 0.002$.

A different behavior is observed when the system is biased along the in-plane hard-axis direction (Fig. 5 for t_{MgO} = 0.72 nm). In this case, the dependence of the precession frequency on the applied field is symmetric and it is weakly influenced by the tunneling barrier thickness. Also in this case the model provides a good reconstruction of the position of the absorption peaks.

V. Conclusion

In summary, MTJ devices, consisting of sputtered CoFeB/MgO/CoFeB layers with MgO layer thickness varying in the range 0.4 nm - 0.98 nm, have been characterized. Both static and dynamic regime have been experimentally investigated by AGFM and VNA-FMR spectroscopy in a wide field range. The MTJ hysteresis loops and the frequency absorption spectra have been measured and their dependence on tunnel barriers thickness has been studied.

Macro-spin models have been developed, enabling the simulation of both the static behavior and the FMR frequency dependence on the bias field, also in presence of strong ferromagnetic coupling between free and reference layers. The different observed behaviors, associated with a variable tunneling barrier thickness, have been correctly reproduced by the theoretical approach, considering external fields applied along both the easy and hard axis direction.

It has been found that for MgO thicknesses lower than 0.6 nm a strong ferromagnetic coupling arises due to impurity-assisted interlayer exchange coupling. This leads to a synchronous reversal of the free and reference layers, which is responsible for the disappearance of the bistable state suitable for STT-MRAM applications. The strong interaction also produces larger asymmetry of the precession frequency with respect to zero field, together with an increase in the effective damping coefficient. Moreover, in the FMR spectrum it is not possible to distinguish the reversal modes corresponding to the frequency precession of the reversal layer, visible in the MTJs with higher tunneling barrier thickness.

The differences in both the static and dynamic behavior strongly reduce when applying the external field along the hard axis direction, orthogonal to exchange bias orientation.

Acknowledgment

This work is supported by the EMRP Joint Research Project IND08 "MetMags".

References

[1] J. A. Katine and E. E. Fullerton, "Device implications of spin-transfer torques", *J. Magn. Magn. Mat*., vol. 320, pp. 1217-1226, 2008.
[2] C. Tiusan et al., "Correlation between micromagnetism and tunnel magnetoresistance in magnetic tunnel junctions using artificial ferrimagnets", *Phys. Rev. B*, pp. 580-593, 2000.
[3] S. Serrano-Guisan et al., "Inductive determination of the optimum tunnel barrier thickness in magnetic tunnelling junction stacks for spin torque memory applications", *J. Appl. Phys*., vol. 110, 023906, 2011.
[4] J. Hayakawa et al., "Current-induced magnetization switching in MgO barrier magnetic tunnel junctions with CoFeB-based synthetic ferrimagnetic free layers", *IEEE Trans. Magn*., vol. 44, pp. 1962-1967, 2008.
[5] C. T. Chao et al., "Coupling strength with off-axial external field in magnetic tunnel junction cells", *J. Appl. Phys*., vol. 109, 07B911, 2011.
[6] D. K. Schreiber et al., "Effects of elemental distributions on the behavior of MgO-based magnetic tunnel junctions", *J. Appl. Phys*., vol. 109, 103909, 2011.
[7] A. Layadi, "Analytical expressions for the magnetization curves of a magnetic-tunnel-junction-like system", *J. Appl. Phys*., vol. 100, 083904, 2006.
[8] K. Yagami, A. A. Tulapurkar, A. Fukushima, and Y. Suzuki, "Low-current spin-transfer switching and its thermal durability in a low-saturation-magnetization nanomagnet", *Appl. Phys. Lett*., vol. 85, 5634, 2004.
[9] S. Ingvarsson, G. Xiao, S. S. P. Parkin, and W. J. Gallagher, "Thickness-dependent magnetic properties of $Ni_{81}Fe_{19}$, $Co_{90}Fe_{10}$ and $Ni_{65}Fe_{15}Co_{20}$ thin films", *J. Magn. Magn. Mat*., vol. 251, pp. 202-206, 2002.
[10] C. Wang et al., "Reduction in critical current density by tuning damping constants of CoFeB for spin-torque-transfer switching", *J. Phys. D: Appl. Phys*., vol. 42, 115006, 2009.
[11] A. V. Silva et al., "Switching field variation in MgO magnetic tunnel junction nanopillars: experimental results and micromagnetic simulations", *IEEE Trans. Magn*., vol. 49, pp. 4405-4408, 2013.
[12] S. S. Kalarickal et al., "Ferromagnetic resonance linewidth in metallic thin films: comparison of measurement methods", *J. Appl. Phys*., vol. 99, 093909, 2006.
[13] J. Smit and H. G. Beljers, "Ferromagnetic resonance absorption in BaFeO, a high anisotropy crystal", *Philips Res. Rep*., vol. 10, pp. 113–130, 1955.
[14] W. Alayo, M. A. Sousa, F. Pelegrini, and E. Baggio-Saitovitch, "Analysis of the weak coupling of the IrMn/Co/Ru/NiFe structures by ferromagnetic resonance", *J. Appl. Phys*., vol. 109, 083917, 2011.
[15] A. Layadi, "Study of the resonance modes of a magnetic tunnel junction-like system", *Phys. Rev. B*, vol. 72, 024444, 2005.
[16] D. H. Kim, H.-H. Kim, C.-Y. You, and H. Kim, "Optimization of ferromagnetic resonance spectra measuring procedure for accurate Gilbert damping parameter in magnetic thin films using a vector network analyzer", *J. Magn*., vol. 16, pp. 206-210, 2011.